

Role of *sn*-1-Saturated,*sn*-2-Polyunsaturated Phospholipids in Control of Membrane Receptor Conformational Equilibrium: Effects of Cholesterol and Acyl Chain Unsaturation on the Metarhodopsin I \leftrightarrow Metarhodopsin II Equilibrium[†]

Drake C. Mitchell, Martin Straume,[‡] and Burton J. Litman*

Department of Biochemistry, University of Virginia Health Sciences Center, Charlottesville, Virginia 22908

Received August 20, 1991; Revised Manuscript Received October 14, 1991

ABSTRACT: The effect of phospholipid bilayer acyl chain packing free volume on the equilibrium concentration of the form of photolyzed rhodopsin which initiates visual signal transduction, metarhodopsin II (meta II), is examined in reconstituted systems formed from the saturated phospholipid dimyristoylphosphatidylcholine (DMPC) and in the polyunsaturated phospholipid *sn*-1-palmitoyl-*sn*-2-arachidonoylphosphatidylcholine (PAPC) with and without 30 mol % cholesterol. The extent of meta II formation is determined from both flash photolysis measurements and rapidly acquired absorbance spectra. Equilibrium and dynamic properties of the lipid bilayer are characterized by the dynamic fluorescence properties of 1,6-diphenyl-1,3,5-hexatriene (DPH). DPH orientational properties are characterized by f_v , a parameter which reflects the volume available for probe reorientation in the bilayer, relative to that available in an unhindered, isotropic environment [Straume, M., & Litman, B. J. (1987) *Biochemistry* 26, 5121-5126]. The metarhodopsin I \leftrightarrow meta II equilibrium constant, K_{eq} has a linear relationship with f_v for rhodopsin in PAPC vesicles with and without cholesterol as well as for rhodopsin in DMPC vesicles, and these two correlation lines have different slopes. The correlations between K_{eq} and f_v in PAPC and DMPC systems are compared with a similar correlation in the native rod outer segment disk membrane and one reported previously in an egg phosphatidylcholine (egg PC) system [Mitchell, D. C., Straume, M., Miller, J. L., & Litman, B. J. (1990) *Biochemistry* 29, 9143-9149]. The slope of the K_{eq} versus f_v correlation line is designated the "permissiveness index", P_i , and is an indicator of the bilayer's capacity to utilize an increase in phospholipid acyl chain packing free volume for accommodation of the expanded meta II conformation. Bilayer cholesterol (up to 30 mol %), in both egg PC and PAPC, reduces both K_{eq} and f_v , but has no effect on P_i . In contrast with the effect of cholesterol, increased unsaturation of the *sn*-2 acyl chain increases P_i . In the DMPC system, P_i is $(6.0 \pm 0.4)K_{eq}f_v^{-1}$; in the egg PC system, it is $(8.4 \pm 1.0)K_{eq}f_v^{-1}$; in the PAPC system, it increases to $(18 \pm 2)K_{eq}f_v^{-1}$; and in the disk membrane, where about 50% of the phospholipid *sn*-2 acyl chains are docosahexaenoyl (22:6), P_i is $(90 \pm 12)K_{eq}f_v^{-1}$. These distinct effects of cholesterol and acyl chain unsaturation on the relationship between K_{eq} and f_v demonstrate that the meta I \leftrightarrow meta II conformational equilibrium may be modulated via bilayer compositional variation. These results suggest a regulatory mechanism which includes a primary role for phospholipid acyl chain composition and a secondary role for bilayer cholesterol content. The reported results demonstrate the potential for detailed regulation of integral membrane receptor function in the essentially isothermal and isobaric environment of a living cell via metabolically controlled changes in phospholipid acyl chain composition and/or cholesterol content of the membrane lipid surrounding the receptor.

In the essentially isothermal and isobaric environment of living cells, the properties of biological membranes may be altered principally by changes in the composition of the membrane. Thus, knowledge of the mechanisms by which lipid bilayer properties and composition modulate the functioning of integral membrane proteins is basic to understanding biological regulation of a major portion of membrane-associated phenomena. Several features of the visual pigment rhodopsin make it uniquely well suited to the study of effects of lipid bilayer properties on integral membrane protein function. Physical studies and analysis of the amino acid sequence in terms of hydropathy plots support a model for rhodopsin consisting of hydrophilic domains linking seven membrane-spanning α -helices with ca. 50% of the mass of the protein

Table I: Values of K_{eq} for Rhodopsin in PAPC, PAPC + 30 mol % Cholesterol, and DMPC^a

temperature (°C)	PAPC	PAPC/30 mol % cholesterol	DMPC ^b
37	3.02 \pm 0.19	1.43 \pm 0.12	0.66 \pm 0.10
30	2.04 \pm 0.11	1.07 \pm 0.10	0.35 \pm 0.08
20	1.15 \pm 0.07	0.61 \pm 0.05	0.06 \pm 0.02
10	0.60 \pm 0.05	0.40 \pm 0.07	c

^a Values of K_{eq} derived as described under Experimental Procedures; uncertainties correspond to one standard deviation. ^b Values from Mitchell et al. (1991a). ^c Not measured.

within the membrane lipid bilayer (Ovchinnikov, 1982; Hargrave et al., 1983). Rhodopsin belongs to a large class of integral membrane receptors that use a G-protein linked to an effector enzyme to couple external stimuli to internal cellular responses. Unique among G-protein-coupled receptors, rhodopsin has covalently bound to it an 11-*cis*-retinal moiety, which is responsible for rhodopsin's photosensitivity and serves as an intrinsic reporter of the protein's functional and con-

[†] Supported by NIH Grant EY00548. A preliminary report of this work appeared in Mitchell et al. (1991b).

* Address correspondence to this author.

[‡] Present address: Biocalorimetry Center, Department of Biology, The Johns Hopkins University, Baltimore, MD 21218.

formational state. Within a few milliseconds of photon absorption, bleached rhodopsin consists of an equilibrium between the metarhodopsin I (meta I)¹ ($\lambda_{\max} = 478$ nm) and meta II ($\lambda_{\max} = 380$ nm) photointermediates (Mathews et al., 1963). Meta II has been shown to be equivalent to ρ^* , the agonist-bound form of the receptor, which is responsible for activation of G_i . Evidence for the correspondence of meta II and ρ^* comes from experimental observations that the binding of G_i to rhodopsin enhances the equilibrium concentration of meta II at the expense of meta I (Eneis et al., 1982) and that the spectrally defined meta II state and the functionally characterized state ρ^* undergo the same rate of thermal decay (Kibelbek et al., 1991). The combination of (1) a rapidly responding, intrinsic reporter of the agonist-bound state, (2) signal transduction by a ubiquitous G-protein activation mechanism, and (3) intimate contact with the phospholipid bilayer makes rhodopsin ideally suited for studying the effects of bilayer composition and physical properties on integral membrane protein function.

The acyl chains of ROS disk membrane phospholipids are highly polyunsaturated, with ~55% of the acyl chains having at least four double bonds (Miljanovich et al., 1979; Drenth et al., 1981). In addition, ~63% of the phospholipids in the ROS disk membrane have saturated acyl chains at the *sn*-1 position and unsaturated acyl chains at the *sn*-2 position (Miljanovich et al., 1979). Cholesterol is a significant component of the ROS disk membrane, with freshly formed disks at the base of the outer segment containing ~26 mol % cholesterol, and mature disks containing ~5 mol % cholesterol (Boesze-Battaglia et al., 1989, 1990). The rod cell plasma membrane contains ~28 mol % cholesterol, and this high level of cholesterol is thought to be responsible for the reduced ability of rhodopsin in the plasma membrane to activate the ROS phosphodiesterase (Boesze-Battaglia & Albert, 1990). The rhodopsin photoreaction cascade has been demonstrated to be sensitive to changes in both cholesterol content and phospholipid acyl chain composition in several reconstituted vesicle systems. In an egg PC bilayer, the presence of 30 mol % cholesterol reduces the equilibrium concentration of meta II by ca. 50% (Mitchell et al., 1990). A sharp reduction in the equilibrium meta II concentration has also been observed for rhodopsin in the saturated phospholipid DMPC (Mitchell et al., 1991a). In contrast, increased formation of meta II for rhodopsin in polyunsaturated phospholipids was reported by O'Brien et al. (1977) and Wiedmann et al. (1988). This enhanced formation of meta II suggests a functional role for the large percentage of polyunsaturated phospholipid acyl chains in the ROS disk membrane.

The present results expand on previous studies from this laboratory to provide an explanation of the dependence of

rhodopsin functional activity on bilayer lipid composition in terms of a critical physical property of the bilayer. Pressure-dependent studies of the meta I–meta II equilibrium have shown that in the meta II state, the rhodopsin–ROS disk membrane system is expanded relative to the meta I state (Attwood & Gutfreund, 1980; Lamola et al., 1974). In addition, DeGrip et al. (1988) have interpreted FTIR measurements as indicating that meta II represents the maximum extent of protein structural alteration in the rhodopsin photointermediate cascade. Thus, it is reasonable to expect that the extent of meta II production in a given lipid bilayer will be correlated with the ability of that bilayer to accommodate significant structural changes associated with an expanded state of the protein.

We have characterized bulk phospholipid acyl chain packing by a parameter, f_v , derived from the fluorescence depolarization behavior of the lipid bilayer probe DPH (Straume & Litman, 1987a). This parameter was developed because intramolecular order parameters, which characterize the conformation of the phospholipid acyl chain, may not directly reflect the global ability of the lipid bilayer to accommodate integral membrane protein conformational changes. We have previously shown that f_v is linearly correlated with the meta I–meta II equilibrium constant, K_{eq} , with regard to perturbation by temperature and/or bilayer cholesterol content in an egg PC bilayer (Mitchell et al., 1990). The present work extends the previous results and establishes similar correlations for rhodopsin in PAPC, DMPC, and the ROS disk membrane. In each of these bilayers, f_v displays the characteristics of a state function of K_{eq} . That is, any combination of temperature and/or bilayer cholesterol that produces a given value of f_v in any given PC system studied yields a unique value of K_{eq} . However, the correlation line representing this linear relationship between K_{eq} and f_v has a unique slope for each acyl chain composition. This slope has been designated the "permissiveness index", P_i , and quantifies the ability of a given bilayer to adjust to the expanded molecular volume of meta II. In DMPC, egg PC, and PAPC reconstituted systems, P_i increases with the degree of acyl chain unsaturation, and in the native ROS disk membrane, which contains ~50% decosahexaenoyl (22:6) acyl chains in its phospholipids (Drenth et al., 1981; Miljanovich et al., 1979), P_i is ca. 5 times larger than in the PAPC system.

EXPERIMENTAL PROCEDURES

Sample Preparation. DMPC and PAPC were purchased from Avanti Polar Lipids Inc. and used without further purification. HPLC analysis, which would detect impurity levels of 0.1% or greater, was carried out by Avanti Polar Lipids Inc. and indicated no detectable impurities in these lipids. Rhodopsin from frozen bovine retinas (Lawson Inc., Lincoln, NE) was solubilized in OG and purified via concanavalin A affinity chromatography (Litman, 1982). Unilamellar vesicles consisting of lyophilized lipid and purified rhodopsin in a molar ratio of 100 to 1, respectively, were prepared using a dilution reconstitution method (Jackson & Litman, 1985), with the modifications of Straume and Litman (1988) regarding the inclusion of cholesterol. The maximum residual OG concentration remaining after this process is ca. 1 molecule of OG per 5000 PC molecules. The partition coefficient for the distribution of OG between a PC bilayer and aqueous buffer is 0.033 mM⁻¹ (Almog et al., 1990); thus, the actual OG:PC ratio in the bilayer was no more than 1:150,000. Concentrated vesicle stock solutions were stored at 4 °C in an isotonic, pH 7.0 buffer consisting of 10 mM PIPES, 60 mM KCl, 30 mM NaCl, 2 mM MgCl₂, and 50 μ M DTPA (PIPES buffer).

¹ Abbreviations: meta I, metarhodopsin I; meta II, metarhodopsin II; DPH, 1,6-diphenyl-1,3,5-hexatriene; ROS, rod outer segment; G_i , visual G-protein, GTPase of the rod outer segment, transducin; PC, phosphatidylcholine; PIPES, piperazine-*N,N'*-bis(ethanesulfonic acid); DTPA, diethylenetriaminepentaacetic acid; OG, octyl glucoside; BHT, butylated hydroxytoluene; PAPC, *sn*-1-palmitoyl-*sn*-2-arachidonoylphosphatidylcholine; DMPC, dimyristoylphosphatidylcholine; K_{eq} , meta I–meta II equilibrium constant, [meta II]/[meta I]; f_v , fractional volume; f_v' , value of f_v where the $K_{eq} - f_v$ correlation line intersects the abscissa; f_l , fraction of DPH oriented parallel to the bilayer in the bimodal orientational distribution model; P_i , permissiveness index, slope of the $K_{eq} - f_v$ correlation line; PS, phosphatidylserine; PE, phosphatidylethanolamine; DAPC, diarachidonoylphosphatidylcholine; SOPC, *sn*-1-stearoyl-*sn*-2-oleoylphosphatidylcholine; POPC, *sn*-1-palmitoyl-*sn*-2-oleoylphosphatidylserine; POPE, *sn*-1-palmitoyl-*sn*-2-oleoylphosphatidylethanolamine; PDPC, *sn*-1-palmitoyl-*sn*-2-decosahexaenoylphosphatidylcholine.

Samples for spectral studies were prepared by diluting the vesicle stock solution with the appropriate temperature-compensated PIPES buffer to a rhodopsin concentration of 0.25–0.35 mg/mL (6.3–8.8 μ M). All measurements were performed on at least three separate sample preparations. The total phospholipid content of the vesicles for each sample preparation was determined by phosphate analysis following the method of Bartlett (1959) and was always within 5% of the desired molar concentration. A cholesterol oxidase assay was used to determine that the total cholesterol content of each sample was within 2 mol % of the desired 30 mol % level (Moore et al., 1977). BHT at a level of 1 molecule per 500 PAPC molecules was added to PAPC stock solutions prior to lyophilization to prevent lipid peroxidation. Lipid peroxidation of PAPC was determined to be less than 0.3% via both 233-nm absorbance and thiobarbituric acid assay (Baker & Wilson, 1969; Slater, 1984; Sunamoto et al., 1985).

Kinetic and Equilibrium Absorbance Measurements. The increase in absorbance at 380 nm following a laser flash ($\lambda = 503$ nm, ca. 15% of the rhodopsin bleached) was monitored with a flash photolysis instrument of our own design (Straume et al., 1990). The meta I \leftrightarrow meta II equilibrium constant, K_{eq} , was derived from the kinetic data via an analysis in terms of a branched photointermediate decay model. The model consists of a branching at meta I into meta II_{fast} and meta II_{slow}, and total meta II = meta II_{fast} + meta II_{slow} (Straume et al., 1990). Meta II_{slow} and meta II_{fast} are kinetically, but not spectrally, resolved, and each is modeled to be in dynamic equilibrium with meta I. The forward and back rate constants of these two equilibria are k_I and k_{II} , respectively, for meta I \leftrightarrow meta II_{fast} and k_A and k_B , respectively, for meta I \leftrightarrow meta II_{slow}. The branched meta II model arises from the consistent requirement for the sum of three exponentials for a statistically valid description of the observed absorbance increase at 380 nm, and has been shown to yield values of K_{eq} which are in good agreement with those derived from equilibrium absorbance spectra (Straume et al., 1990; Mitchell et al., 1990, 1991a).

Deconvolved difference spectra of meta I \leftrightarrow meta II equilibrium mixtures were derived from a series of four absorbance spectra acquired with a Hewlett-Packard 8452A diode array spectrophotometer (0.2-s measuring time yielded <0.3% bleach by measuring beam). These include (1) the initial rhodopsin-containing vesicle suspension, (2) 3 s after a brief strobe flash which passed through a (520 \pm 25)-nm band-pass filter (15–20% bleach), (3) following addition of 2 M hydroxylamine to yield a final concentration of 30 mM, and (4) after complete bleaching of the sample. Difference spectra consisting of the equilibrium mixture of meta I and meta II present 3 s after bleaching were constructed by subtracting curve 1 from curve 2 and adding to this difference spectrum the spectrum of the bleached rhodopsin. Individual meta I and meta II spectra were deconvolved from the spectrum of their equilibrium mixture by nonlinear least-squares estimation of the sum of two asymmetric quasi-Gaussians, one for meta I and one for meta II. Concentrations of meta I and meta II were calculated using extinction coefficients of 44 000 cm⁻¹ M⁻¹ for meta I and 38 000 cm⁻¹ M⁻¹ for meta II (Applebury, 1984). Additional details regarding acquisition and analysis of both kinetic and equilibrium spectral data may be found in Straume et al. (1990).

Fluorescence Measurements. Vesicle samples were diluted to 0.5 mM phospholipid and labeled to 250:1 (mol/mol) phospholipid/DPH. Samples were equilibrated at 37 °C in an SLM-4800 limited-frequency phase-modulation dynamic

spectrofluorometer, and steady-state and dynamic measurements were performed at 37, 25, 15, and 5 °C. Excitation was at 360 nm passed through 1-nm slits, and emission was monitored at 430 nm after passage through 16-nm slits. Steady-state anisotropies were corrected for all instrumental factors. All dynamic measurements were made relative to a POPOP/absolute ethanol reference solution (Lakowicz, 1980). Rhodopsin in the samples experienced no detectable bleaching as a result of the measurements. Additional details regarding the fluorescence measurements may be found in Straume and Litman (1987a).

Analysis of DPH Fluorescence. Total fluorescence intensity decay behavior was analyzed according to a biexponential model of DPH lifetime behavior imposing the constraint that $\tau_2 = 4\tau_1$. This constraint imposed on the $\tau_2:\tau_1$ ratio was derived from numerous reports in the literature based on lifetime behavior obtained from biexponential analysis of DPH in bilayers [see, for example, Ameloot et al. (1984), Chen et al. (1977), Hildenbrand and Nicolau (1979), Kawato et al. (1977), Kinoshita et al. (1981a,b), Klausner et al. (1980), Lakowicz et al. (1985), Parasassi et al. (1984), and Stubbs et al. (1981, 1984)]. Rotational depolarization of DPH was characterized by means of a bimodal equilibrium orientational distribution model for this fluorophore (Ameloot et al., 1984; van de Ven et al., 1984; Vogel & Jahnig, 1985; Vos et al., 1983). This model characterizes DPH equilibrium orientational properties by (1) the width of the Gaussian distribution of the orientational probability, θ_g , (2) the fraction of the probe occupying the orientational probability maximum parallel to the bilayer normal, $f_{||}$, and (3) the perpendicular rotational diffusion coefficient, D_{\perp} (Straume & Litman, 1987a,b). Overall equilibrium ordering experienced by DPH was quantified by the parameter f_v , which characterizes the volume available for probe reorientational motion in the anisotropic bilayer relative to that available in an unhindered, isotropic environment. This parameter is defined as

$$f_v = \frac{\int f(\theta) \sin \theta d\theta}{2f(\theta)_{\max}}$$

where $f(\theta)$ is a function of θ_g and $f_{||}$. Thus, f_v makes possible direct comparison of average phospholipid acyl chain equilibrium ordering among systems and under conditions where $f_{||}$ varies, eliminating the need for simultaneous interpretation of θ_g and $f_{||}$.

All parameter estimation in the course of analysis of both absorbance and fluorescence measurements was performed by application of a modified Gauss–Newton nonlinear least-squares algorithm (Johnson, 1983; Johnson & Frasier, 1985). Analysis of K_{eq} as a function of f_v , where there is statistically significant uncertainty in both the independent and dependent variables, was performed by application of a Nelder–Mead least-squares algorithm which explicitly accounts for uncertainty in both independent and dependent variables (Johnson, 1985). Asymmetrical confidence intervals corresponding to one standard deviation were estimated by both parameter estimation algorithms, but due to the minimal observed asymmetry, a single value of uncertainty corresponding to one standard deviation is reported for all derived quantities.

RESULTS

Absorbance Measurements. Flash photolysis measurements were performed to examine the dynamics of establishment of the meta I \leftrightarrow meta II equilibrium and to determine K_{eq} in PAPC vesicles with and without 30 mol % cholesterol as a function of temperature. In addition, K_{eq} was also determined

Table II: Effects of Bilayer Composition on both K_{eq} and the Rate Constants of Meta I \leftrightarrow Meta II for the Branched Meta II Model at 37 °C, pH 7.0^a

bilayer composition	K_{eq}	meta I \leftrightarrow meta II _{fast}		meta I \leftrightarrow meta II _{slow}	
		k_I	k_{II}	k_A	k_B
ROS disk membrane ^b	7.3 ± 0.6	0.34 ± 0.03	0.52 ± 0.18	0.48 ± 0.02	0.072 ± 0.005
PAPC	3.0 ± 0.2	0.25 ± 0.03	0.77 ± 0.18	0.27 ± 0.07	0.098 ± 0.01
egg PC ^c	1.0 ± 0.1	0.14 ± 0.003	0.74 ± 0.03	0.13 ± 0.02	0.16 ± 0.007
DMPC ^d	0.66 ± 0.1	0.144 ± 0.002	0.62 ± 0.02	0.039 ± 0.003	0.104 ± 0.004
PAPC/30 mol% chol	1.43 ± 0.12	0.17 ± 0.01	1.02 ± 0.03	0.24 ± 0.02	0.19 ± 0.003
egg PC/30 mol% chol ^e	0.55 ± 0.03	0.093 ± 0.01	1.01 ± 0.02	0.113 ± 0.004	0.25 ± 0.01

^a Values of K_{eq} derived from kinetic absorbance measurements following analysis in terms of the branched meta II model. All rate constants are in ms^{-1} . The rate constants of the meta I \leftrightarrow meta II portion of the branched meta II model at 37 °C, pH 7.0, were derived following the methods outlined in Straume et al. (1990). k_I is the forward rate meta I \rightarrow meta II_{fast}, k_{II} is the back rate meta I \leftarrow meta II_{fast}, k_A is the forward rate meta I \rightarrow meta II_{slow}, and k_B is the back rate meta I \leftarrow meta II_{slow}. ^b Data for ROS disk membranes from Straume et al. (1990). ^c Data for egg PC are from Mitchell et al. (1990). ^d Data for DMPC are from Mitchell et al. (1991a).

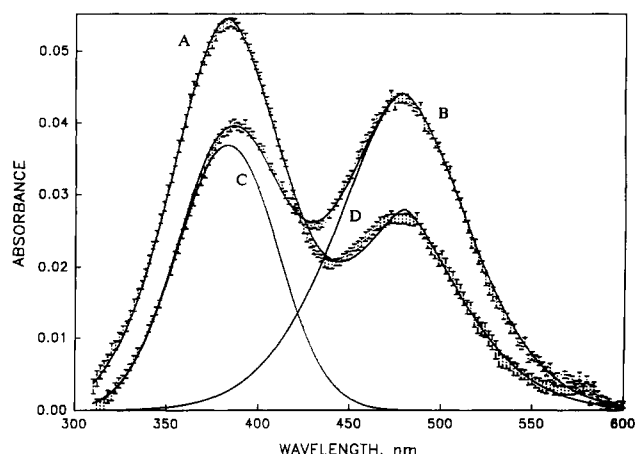


FIGURE 1: Corrected difference spectra of the meta I \leftrightarrow meta II equilibrium for photolyzed rhodopsin in PAPC vesicles containing 0 (A) and 30 (B) mol % cholesterol in pH 7.0 PIPES buffer at 30 °C. Spectra were normalized to the same concentration of photolyzed rhodopsin; thus, the shift in relative meta I–meta II peak heights indicates the shift in the meta I \leftrightarrow meta II equilibrium induced by 30 mol % cholesterol. Points with error bars are corrected difference spectra; smooth curves through points are the best fit of the sum of two asymmetric, quasi-Gaussian functions to the difference spectra. Deconvolved individual spectra of meta II (C) and meta I (D) for the 30 mol % cholesterol spectrum are shown as solid curves.

by deconvolving the individual meta I and meta II absorbance bands from difference spectra consisting of meta I and meta II in equilibrium. The values of K_{eq} derived from these two techniques were identical within experimental error, at all four temperatures (comparison of K_{eq} 's not shown). Correspondence between K_{eq} 's determined kinetically and from equilibrium difference spectra was previously demonstrated in studies involving ROS disk membranes (Straume et al., 1990), and for rhodopsin in egg PC (Mitchell et al., 1990) and DMPC vesicles (Mitchell et al., 1991a). All values of K_{eq} reported in this study were derived from flash photolysis measurements. The values of K_{eq} at 10, 20, 30, and 37 °C for rhodopsin in PAPC bilayers with and without 30 mol % cholesterol (Table I) show that the effect of cholesterol on the extent of meta II formation in PAPC vesicles is qualitatively similar to that previously observed in egg PC vesicles (Mitchell et al., 1990). At all four temperatures, 30 mol % cholesterol reduced K_{eq} by approximately 50%, the same degree of reduction observed for 30 mol % cholesterol in an egg PC bilayer. The cholesterol-induced reduction in the equilibrium meta II concentration in a PAPC bilayer at 30 °C, pH 7.0, is shown graphically by the deconvolved difference spectrum in Figure 1. The change in peak absorbances of the deconvolved individual bands for meta I and meta II clearly shows that 30 mol % cholesterol induces a redistribution of the meta I–meta II equilibrium in favor of

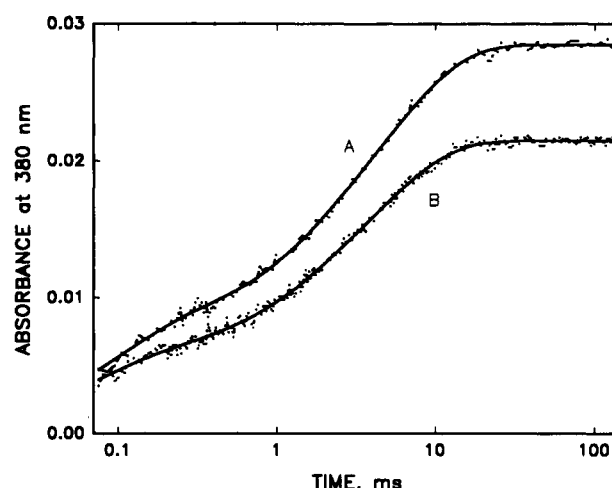


FIGURE 2: Increase in absorbance at 380 nm for photolyzed rhodopsin in PAPC vesicles containing 0 (A) and 30 (B) mol % cholesterol in pH 7.0 PIPES buffer at 37 °C. Data normalized to the same concentration of photolyzed rhodopsin are shown as points; solid curves are the best fit of the branched meta II model to the data.

meta I. A comparison of the amplitudes of the normalized kinetic absorbance curves, shown in Figure 2, also demonstrates the reduction in meta II formation produced by 30 mol % cholesterol. Cholesterol also has a similar effect in both PAPC and egg PC vesicles on the kinetics of meta II_{fast} and meta II_{slow} derived from the branched decay model (see Experimental Procedures). The two forward rates, k_I and k_A , are decreased, and the two reverse rates, k_{II} and k_B , are increased by 30 mol % cholesterol in both PAPC and egg PC vesicles, as shown in Table II. At 37 °C, 30 mol % cholesterol decreases k_I and k_A by 31% and 9%, respectively, in PAPC bilayers and by 34% and 13%, respectively, in egg PC bilayers. The two reverse rates, k_{II} and k_B , are increased at 37 °C by 30 mol % cholesterol by 32% and 94%, respectively, in PAPC bilayers and by 36% and 54%, respectively, in egg PC bilayers. Thus, in both PAPC and egg PC bilayers, cholesterol reduces the rate of overall meta II formation and has a greater effect on the reverse rates of meta I \leftrightarrow meta II_{fast} and meta I \leftrightarrow meta II_{slow} than on the forward rates, particularly with regard to the meta I \leftrightarrow meta II_{slow} equilibrium.

In the lipid bilayers we have studied to date, the rates of formation of both meta II_{fast} and meta II_{slow} increase in the following order: DMPC < egg PC < PAPC < ROS disk membrane. In all of these bilayers, at least two-thirds of equilibrium meta II consists of meta II_{slow}. Since meta II_{slow} is the predominant pathway in these bilayers, the kinetics of meta II_{slow} have the greater influence on the total system, and the rate of meta II formation is dominated by k_A . This rate constant has a wide range of values at 37 °C in PAPC, egg

Table III: Comparison of DPH Fluorescence Properties in Rhodopsin-Containing DMPC and PAPC Vesicles: Intensity-Weighted Mean Fluorescence Lifetimes and f_v^a

tempera- ture (°C)	DMPC		PAPC ^b	
	$\tau(1)$ (ns)	f_v	$\tau(1)$ (ns)	f_v
37	4.79 ± 0.55	0.129 ± 0.005	2.40 ± 0.07	0.198 ± 0.033
30	5.75 ± 0.70	0.095 ± 0.002	c	
28	6.09 ± 0.22	0.074 ± 0.014	c	
26	6.37 ± 0.66	0.059 ± 0.024	c	
25	c		2.57 ± 0.10	0.150 ± 0.037
24	6.99 ± 0.51	0.047 ± 0.002	c	
22	7.66 ± 0.35	0.039 ± 0.002	c	
20	8.12 ± 0.43	0.035 ± 0.005	c	
15	8.70 ± 0.66	0.028 ± 0.005	2.83 ± 0.08	0.173 ± 0.029
6	9.15 ± 0.60	0.022 ± 0.005	3.32 ± 0.20	0.070 ± 0.006

^aAll uncertainties correspond to one standard deviation. ^bValues from the appendix to Straume and Litman (1988). ^cNot measured.

PC, and DMPC vesicles, and in ROS disk membranes, as shown in Table II. The value of k_A in ROS disk membranes is ~12 times larger than in DMPC and 1.8 times larger than in PAPC. The reduction in equilibrium meta II concentration, when compared with the native disk membrane, also increases with saturation of the acyl chain at the *sn*-2 position of the phospholipid. The values of K_{eq} shown in Table II correspond to an equilibrium mole fraction for meta II of 0.88 in ROS disk membranes, and 0.75, 0.5, and 0.4 in PAPC, egg PC, and DMPC vesicles, respectively. Thus, for the pure phospholipid bilayers, there is a strict correlation between phospholipid acyl chain compositions which promotes both the extent and rate of formation of meta II.

Fluorescence Measurements. Equilibrium phospholipid acyl chain packing was quantified in terms of the parameter f_v , which was derived from the dynamic fluorescence depolarization of DPH. The temperature dependence of the fluorescence lifetime and rotational reorientation of DPH in rhodopsin-containing DMPC vesicles was measured. The sensitivity of DPH fluorescence properties to the characteristics of the lipid bilayer is made apparent by comparing the fluorescence lifetimes measured in DMPC with those obtained earlier in similar vesicles of PAPC (Straume & Litman, 1988) (Table III). At all temperatures, the intensity-weighted mean fluorescence lifetime, $\tau(1)$, is a factor of 2–3 greater in DMPC than in PAPC, as shown in Table III. A second major difference in DPH fluorescence lifetime behavior between these two lipid bilayers is the effect of temperature. A reduction in temperature from 37 to 5 °C increases $\tau(1)$ by a factor of 2 in DMPC, but raises $\tau(1)$ by less than 50% in PAPC. These differences in fluorescence lifetimes for DPH in DMPC and PAPC are thought to be due in part to greater penetration of water molecules into the PAPC bilayer, and demonstrate the sensitivity of DPH to the physical state of the lipid bilayer.

DPH is a linear, symmetric molecule; thus, its equilibrium orientational properties are expected to closely reflect the degree of ordering of the phospholipid acyl chains of the bilayer. The gel and liquid-crystalline phases constitute two extreme states of acyl chain ordering. The gel-to-liquid-crystalline transition in a rhodopsin-containing DMPC bilayer is fairly broad with a T_m of approximately 23–24 °C (Hong & Hubbell, 1972). This phase behavior is reflected by the temperature dependence of the fraction of DPH oriented parallel to the membrane normal, $f_{||}$, which is derived from the bimodal analysis of the fluorescence depolarization data (Straume & Litman, 1987a, and see *Analysis of DPH Fluorescence* under Experimental Procedures) and the fractional volume, f_v , as shown in Figure 3. For the three temperatures well below T_m , 5, 15, and 20 °C, $f_{||}$ is greater than

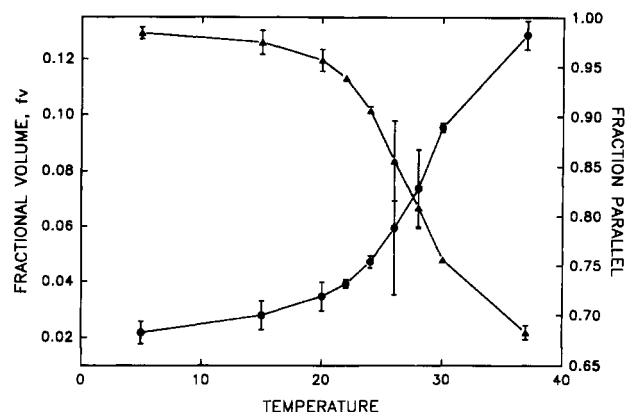


FIGURE 3: Effects of temperature on f_v (●) and $f_{||}$ (▲) for DPH in rhodopsin-containing DMPC vesicles in pH 7.0 PIPES buffer. Error bars correspond to one standard deviation; points without error bars have a standard deviation smaller than the symbol. See *Analysis of DPH Fluorescence* under Experimental Procedures for an explanation of f_v and $f_{||}$.

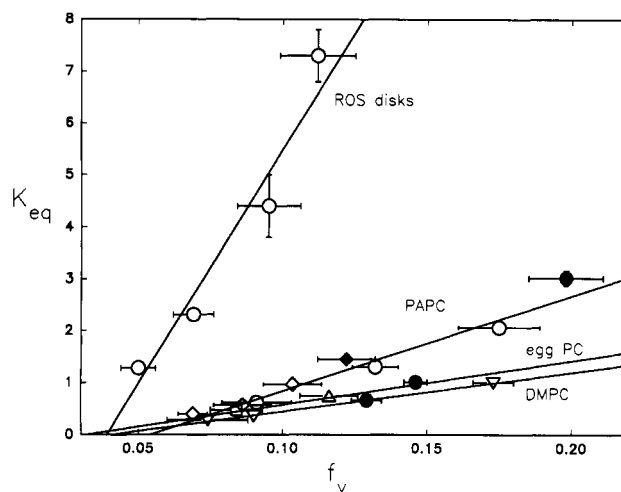


FIGURE 4: Correlation of K_{eq} and f_v for all bilayer compositions. All solid circles (●) denote 37 °C values in pure phospholipid bilayers and illustrate the variation in both parameters resulting strictly from variation of the phospholipid acyl chain composition. PAPC/30 mol % cholesterol at 10, 20, and 30 °C (◊); PAPC/30 mol % cholesterol at 37 °C (◆); egg PC/15 mol % cholesterol at 37 °C (Δ); egg PC/30 mol % cholesterol at 37 °C (◻); DMPC at 27, 30, and 45 °C (▼). Temperatures for ROS disks and PAPC vesicles are 10, 20, 30, and 37 °C. The correlation line for egg PC was derived from 12 points [10, 20, 30, and 37 °C for 0, 15, and 30 mol % cholesterol (Mitchell et al., 1990)], but for simplicity, only the 37 °C points are shown for each of the 3 cholesterol levels. Error bars correspond to one standard deviation; points without error bars have standard deviation smaller than the symbol.

0.95, and f_v is only moderately elevated by an increase in temperature from 5 to 20 °C. In the vicinity of the phase transition, 20–30 °C, both f_v and $f_{||}$ change rapidly with temperature. Above 30 °C, the probability distribution oriented parallel to the bilayer normal continues to decrease, yielding values of $f_{||} < 0.75$. Under these conditions, f_v increases. At temperatures above T_m , the width of the orientational probability distribution for DPH about each of its orientational axes, θ_g , broadens significantly (data not shown), and the two orientational distributions become more equally populated. This behavior is consistent with increasing disorder in the median region of the bilayer, resulting from the gel-to-liquid-crystalline phase transition, and demonstrates that the rotational reorientation of DPH, as quantified by f_v and $f_{||}$, reflects the average order of the phospholipid acyl chains.

Correlation of K_{eq} and f_v . The effects of the physical state of the lipid bilayer on K_{eq} in PAPC and DMPC vesicles were determined by examining the dependence of K_{eq} on f_v . Data

Table IV: Slopes and x Intercepts of K_{eq} vs f_v Correlation Lines^a

parameter	ROS disk membrane	PAPC	egg PC	DMPC
slope (P_i)	90 ± 12	18 ± 2	8.4 ± 1.2	6.0 ± 0.4
x intercept (f_v')	0.039 ± 0.008	0.05 ± 0.01	0.032 ± 0.009	0.042 ± 0.003

^a All parameters and uncertainties corresponding to one standard deviation derived using least-squares analysis which accounts for the uncertainty in both dependent and independent variables (Johnson, 1985).

for rhodopsin in PAPC bilayers, with 0 and 30 mol % cholesterol, fell on a single correlation line, demonstrating a linear relationship between K_{eq} and f_v over the temperature range 10–37 °C, as shown in Figure 4. The solid circle and solid diamond on the PAPC line in Figure 4 denote measurements made at 37 °C, and represent the isothermal variation in both parameters resulting exclusively from the influence of 30 mol % cholesterol. The correlation shown in Figure 4 for PAPC demonstrates that whether the composition of the bilayer is isothermally modified or the temperature is varied at a given bilayer composition, the linear relationship between K_{eq} and bilayer phospholipid acyl chain packing free volume, as quantified by f_v , remains unchanged. Data for rhodopsin in DMPC bilayers from 5 to 45 °C also fall on a single correlation line. However, the linear correlation was significantly improved by including only temperatures above T_m (27, 30, 37, and 45 °C), and these are shown in Figure 4. The results for rhodopsin in PAPC and DMPC vesicles summarized in Figure 4 show that the parameter f_v is well correlated with the extent of an integral membrane protein conformational equilibrium, in both a saturated and a polyunsaturated lipid bilayer. We previously observed a similar linear correlation between K_{eq} and f_v for rhodopsin in egg PC vesicles with 0, 15, and 30 mol % cholesterol (Mitchell et al., 1990), and this correlation line is shown in Figure 4. In order to determine whether the production of meta II in the native ROS disk membrane is correlated with f_v , values of K_{eq} (Straume et al., 1990) and f_v (Straume & Litman, 1988) for rhodopsin in ROS disks at 10, 20, 30, and 37 °C are also plotted in Figure 4. The resulting $K_{eq} - f_v$ correlation line demonstrates the high sensitivity of the metarhodopsin equilibrium to changes in the phospholipid acyl chain packing free volume in the native ROS disk membrane. The slope of the correlation line was designated as the "permissiveness index", P_i , because it quantifies the extent to which a given bilayer can accommodate the expanded molecular volume of meta II, thus allowing increased meta II production, for a given increase in f_v . For the four bilayers shown in Figure 4, the P_i increases with increasing acyl chain unsaturation, as shown in Table IV. The ROS disk membrane P_i is 5 and 15 times greater than that of rhodopsin in PAPC and DMPC vesicles, respectively. The intercept of each line with the abscissa, f_v' , indicates a threshold value of f_v , which must be achieved before meta II formation can occur. Although slopes of the four lines in Figure 4 have a wide range of values, all of these systems share a common value for f_v' of about 0.04, as shown in Table IV. The results presented in Figure 4 and Table IV demonstrate that while systems may share a common value of f_v' for a particular integral membrane protein conformational change, they differ widely in their ability to absorb the volume change associated with the meta I to meta II transition.

DISCUSSION

Organisms live under essentially isothermal and isobaric conditions. As such, control of the physical properties of the

membranes of these organisms must be via metabolic regulation of their membrane composition. The vast majority of membrane function is related to membrane proteins. Many of these proteins are integral membrane proteins, having a significant portion of their mass within the bilayer. These proteins generally need to undergo an activating conformational change to become functionally competent; this change likely involves an activated conformation of increased volume and would include the opening of a ligand or substrate binding cleft or a channel or pore. A major goal of this research is to describe a physical property of biological membranes which correlates with the extent of a functionally relevant integral membrane protein conformational change. This property must have the characteristic of responding to bilayer compositional changes at constant temperature and pressure, thus demonstrating its potential to respond to metabolic control of membrane lipid composition. We find that such a property is the phospholipid acyl chain packing free volume, as quantified by f_v . This parameter demonstrates the requisite correlation with the K_{eq} for the meta I \leftrightarrow meta II transition of rhodopsin with respect to both temperature and compositional variation. For a given phospholipid composition, f_v has the characteristic of a thermodynamic state function, in that the system responds to the attainment of a specific f_v value, whether reached via variation of composition or temperature, by yielding the same K_{eq} for the meta I \leftrightarrow meta II transition. The range of values of K_{eq} and f_v , which may be realized via isothermal variation of bilayer phospholipid acyl chain composition is shown by the filled circles in Figure 4. Since these symbols correspond to measurements made at 37 °C in pure phospholipid bilayers, they demonstrate the changes in the conformational equilibrium and acyl chain packing free volume which can be solely attributed to changes in acyl chain unsaturation, while maintaining a phosphatidylcholine headgroup.

The current results provide a clear demonstration of the potential for control of integral membrane protein conformation, and hence function, by variation in membrane composition. These results also suggest a dual mechanism for such metabolic control and a rationale for what is by far the most common motif in membrane phospholipid structure: the presence of a saturated and an unsaturated acyl chain in the *sn*-1 and *sn*-2 position, respectively. The first level of control results from the mix of phospholipid acyl chain composition at the *sn*-1 and *sn*-2 positions. This is demonstrated by the increasing slope of the correlation lines (larger values of P_i) with increasing degree of unsaturation at the *sn*-2 position, showing that increasing unsaturation is associated with more permissive bilayer properties with respect to the protein conformational change (Figure 4 and Table IV). This broad level of control is also reflected in the fact that K_{eq} and f_v show an increasing range of values, for the same temperature interval, with increasing acyl chain unsaturation. Thus, the unsaturation level of the *sn*-2 acyl chain establishes the extent to which integral membrane protein conformational equilibria will be able to respond to subtle changes in acyl chain packing. The second level of control is a "fine tuning" of the membrane phospholipid acyl chain packing free volume, which results from the addition of other lipids to the bilayer such as cholesterol. Cholesterol changes f_v and moves the system along the correlation line determined by the host lipid. Alterations in bilayer cholesterol content do not change the basic relationship between K_{eq} and f_v for a given phospholipid bilayer. The incorporation of cholesterol leaves P_i unchanged but has the effect of moving the system to a new point along the particular $K_{eq} - f_v$ correlation line. This aspect of the effect

of cholesterol suggests a specific regulatory role for cholesterol in biological membranes which is related to its effect on the phospholipid acyl chain packing free volume. Changes in bilayer cholesterol could provide a mechanism for isothermally fine-tuning integral membrane protein conformational equilibria. These two levels of compositional control mean that an organism could alter integral membrane protein conformational equilibria to a large degree, or maintain the physical conditions required for membrane protein function, by varying the phospholipid acyl chain composition, or to a more subtle degree by varying the membrane composition with respect to a lipid such as cholesterol. Thus, the results summarized in Figure 4 demonstrate two distinct mechanisms for potential isothermal regulation of integral membrane protein functionality by changes in the composition of the lipid bilayer.

The necessity of the *sn*-1, *sn*-2 acyl chain compositional motif in the regulatory mechanism described above is further evidenced by the following studies. Needham and Nunn (1990) have demonstrated that a bilayer composed of DAPC has a low degree of cohesiveness and can undergo a relatively large change in surface area in response to a relatively low applied stress, indicating a fragile, but highly compressible bilayer. Addition of cholesterol to these bilayers has relatively little effect on the bulk bilayer properties. In contrast, bilayers formed of SOPC are more cohesive than DAPC bilayers and undergo smaller changes in surface area in response to a larger applied stress. Addition of saturating levels of cholesterol to SOPC bilayers greatly decreased bilayer area compressibility and greatly increased bilayer strength. DMPC bilayers were shown to be both stronger and relatively incompressible, when compared to DAPC, and to become less compressible with increasing cholesterol content (Evans & Needham, 1987). Hence, acyl chain polyunsaturation results in high area compressibility and weak bilayers, whereas phospholipid acyl chain saturation results in lower area compressibility and increased strength. A combination of these two types of acyl chains, as is found in natural membranes, would be expected to contribute both these required features to the physical nature of biological membranes. In addition, two independent experimental results indicate that the fine adjustment of bilayer properties, via membrane cholesterol content, would require the presence of a saturated acyl chain. The compressibility of phospholipids with two polyunsaturated chains (DAPC) is relatively unaltered by cholesterol (Needham & Nunn, 1990). The lack of interaction between cholesterol and polyunsaturated acyl chains is also evidenced by the fact that cholesterol is reported to have no effect on the thermal melting behavior of dipolyunsaturated PCs (Kariel et al., 1991).

The effects of cholesterol on the kinetics of meta II formation support the idea that cholesterol interacts predominantly with the saturated *sn*-1 acyl chain. Table II shows that in PAPC and egg PC, cholesterol has a very similar effect on all four of the rate constants of the meta I \leftrightarrow meta II equilibrium. The presence of the polyunsaturated (20:4) acyl chain at the *sn*-2 position in PAPC produces no changes in the effects of cholesterol on these kinetic processes previously observed in egg PC. This implies that cholesterol influences the kinetics of meta II formation via interaction with the saturated acyl chain at the *sn*-1 position.

In earlier studies, the dynamic fluorescence properties of the membrane bilayer probe DPH were used to characterize the effects of cholesterol, unsaturation at the *sn*-2 position, incorporation of the integral membrane protein rhodopsin, and temperature on phospholipid acyl chain packing properties (Straume & Litman, 1988, 1987a,b). It was shown in these

studies that in rhodopsin-containing systems, the observed DPH fluorescence is substantially weighted toward DPH molecules in the bulk lipid rather than from DPH molecules in the lipid-protein interfacial region. This is due to the fact that the retinal chromophore of rhodopsin is an efficient quencher of DPH fluorescence via energy transfer. In addition, measurements were made on vesicle systems incorporating rhodopsin which had been bleached and the retinal chromophore removed, yielding a system in which fluorescence could be observed from DPH molecules both in the bulk bilayer and in the lipid-protein interfacial region. These experiments yielded parameter values characteristic of the equilibrium order and dynamics of DPH rotational diffusion identical with those derived for native rhodopsin vesicle systems (Straume & Litman, 1988). This result demonstrates that DPH depolarization properties reflect the equilibrium acyl chain packing of the bulk lipid of the bilayer rather than boundary lipid at the lipid-rhodopsin interface.

DPH depolarization properties have been analyzed using a bimodal distribution model, and the fractional volume parameter, f_v , was determined by integrating the normalized orientational distribution function in order to quantify the degree of overall system ordering in terms of a single parameter. This parameter describes the relative volume available to the probe for reorientational motion in an anisotropic bilayer compared with that available in a system which allows an isotropic, spherically symmetric distribution. Since f_v contains both orientational distribution and distribution width information, it provides a convenient means for quantitatively comparing acyl chain equilibrium ordering by a single parameter regardless of sample composition or temperature. Unlike intramolecular order parameters, which report on the conformation of individual acyl chains, f_v reflects the average motional properties of DPH in a way that characterizes the packing properties of an ensemble of lipid molecules in the bilayer. The correlations presented in Figure 4 demonstrate that for a given phospholipid composition, f_v has the characteristics of a state function of K_{eq} with regard to variation in temperature and bilayer cholesterol content.

Comparison of the effects of bilayer cholesterol and temperature on f_v with the reported effects of these perturbations on bilayer thickness makes it possible to assess the extent to which changes in f_v reflect changes in bilayer thickness. An increase in f_v implies an increase in volume in the hydrophobic core of the bilayer, which could be derived from an increase in bilayer thickness or a reduction in phospholipid lateral packing. In pure egg PC vesicles, f_v increases sharply with temperature from 5 to 37 °C ($\Delta f_v/\Delta T = 0.005$), while in egg PC vesicles with 30 mol % cholesterol f_v increases more weakly with temperature over this temperature range [$\Delta f_v/\Delta T = 0.001$; data from Straume and Litman (1987b)]. Sankaram and Thompson (1990) have recently shown in a series of disaturated PC's, both with and without cholesterol, that fluid-phase bilayers thin slightly with increasing temperature. Thus, in lipid bilayers with and without cholesterol, bilayer thickness decreases with temperature over a temperature range where f_v increases. This comparison appears to rule out the possibility that changes in f_v are directly correlated with changes in bilayer thickness and makes it more likely that the changes in phospholipid acyl chain packing free volume quantified by f_v are related to changes in lateral packing of the phospholipid headgroups.

Increased levels of phospholipid acyl chain unsaturation produce greater values of P_i , as shown in Figure 4 and Table IV. However, the ~ 5 -fold disparity between P_i for the ROS

disk membrane and a PAPC bilayer suggests that additional factors may contribute to the high permissiveness index in the ROS disk membrane. Several unique features of the ROS disk membrane may be responsible for its having a higher value of P_i . The phospholipids of the disk membrane include a high proportion of PE and PS headgroups in addition to PC, and these are thought to be asymmetrically distributed between the two monolayers of the disk membrane bilayer (Smith et al., 1975). It was reported that higher equilibrium concentrations of meta II are attained as the ratio of POPS or POPE to POPC is increased in rhodopsin-containing reconstituted vesicles (Mone & Litman, 1991). In addition, the disk membrane contains a high percentage of decosahexaenoyl (22:6) acyl chains; thus, an analysis of K_{eq} vs f_v for rhodopsin in vesicles containing decosahexaenoyl acyl chains would be required to assess the contribution of acyl chain polyunsaturation to the high P_i values observed in the disk membrane. However, the results reported here strongly suggest that the high level of decosahexaenoyl acyl side chains in the disk membrane serves a structural role, imparting to the disk membrane properties which promote the formation of meta II, thus enhancing the signal transduction pathway.

The meta II photointermediate has been shown to be the functionally active form of the integral membrane receptor rhodopsin which activates the visual G-protein transducin (Emeis et al., 1982; Kibelbek et al., 1991). Meta II is in equilibrium with meta I and has been shown to be expanded relative to meta I (Lamola et al., 1974; Atwood & Gutfreund, 1980). Time-resolved FTIR measurements have been interpreted as showing changes in the overall shape of rhodopsin at the meta II stage due to slight rearrangement of α helices (DeGrip et al., 1988). The correlation between K_{eq} and f_v suggests that a significant component of the conformational change associated with meta II is radially outward, in the plane of the bilayer. The meta I \leftrightarrow meta II conformational equilibrium of rhodopsin, as characterized by K_{eq} , and the packing free volume of the lipid acyl chains, as characterized by f_v , have been shown to be linearly correlated for rhodopsin in the native ROS disk membrane and in PC bilayers of phospholipids comprised of varying acyl chain compositions and cholesterol content. The slope of this correlation line increases with unsaturation of the phospholipid acyl chains, and this may be related to the presence of microdomain formation in bilayers composed of highly unsaturated phospholipids. Raman spectral studies suggest that PAPC and PDPC bilayers have a microdomain structure in the liquid-crystalline phase (Litman et al., 1991). It is possible that changes in domain size could play a role in allowing the expansion of an integral membrane protein. The x intercept of K_{eq} vs f_v , f_v' , does not depend strongly on the composition of the bilayer, as shown in Table IV. The similar values of f_v' for the various phospholipid systems suggest that a universal minimum or threshold value of f_v is required for formation of meta II regardless of the composition of the lipid bilayer. This requirement may be related to the nature of the molecular volume expansion involved in the transition from meta I to meta II. The slope of the K_{eq} vs f_v line, on the other hand, reflects the packing properties of a given phospholipid acyl chain composition, which enable it to rearrange the acyl chains and accommodate the conformational change associated with meta II formation. The effect of cholesterol is to move the conformational equilibrium along a particular correlation line, thus suggesting a more subtle regulatory function for bilayer cholesterol. A suggested mechanism for this action is the effect of cholesterol in reducing the packing free volume of phospholipid acyl

chains, as indicated by the observed variation in f_v . Taken together, the effects of variation of acyl chain unsaturation at the *sn*-2 position and variation of bilayer cholesterol content clearly delineate a dual level of control for the isothermal and isobaric modulation of integral membrane protein conformational equilibria by metabolic control of lipid bilayer composition.

ACKNOWLEDGMENTS

We thank Lisa Miller and Deborah Stokes for help in preparing the recombinant vesicles and performing the associated assays. We also thank Dr. Michael L. Johnson for making available his nonlinear least-squares parameter estimation programs and for much helpful advice regarding data analysis.

Registry No. DMPC, 18194-24-6; PAPC, 35418-58-7; cholesterol, 57-88-5.

REFERENCES

- Almog, S., Litman, B. J., Wimley, W., Cohen, J., Wachtel, E. J., Barenholz, Y., Ben-Shaul, A., & Lichtenberg, D. (1990) *Biochemistry* 29, 4582-4592.
- Ameloot, M., Hendrickx, H., Herreman, W., Pottel, H., van Cauwelaert, F., & van der Meer, W. (1984) *Biophys. J.* 46, 525-539.
- Applebury, M. L. (1984) *Vision Res.* 24, 1445-1454.
- Applebury, M. L., Zuckerman, D. M., Lamola, A. A., & Jovin, T. M. (1974) *Biochemistry* 13, 3448-3458.
- Attwood, P. V., & Gutfreund, H. (1980) *FEBS Lett.* 119, 323-326.
- Baker, N., & Wilson, L. (1966) *J. Lipid Res.* 7, 341-348.
- Bartlett, G. R. (1959) *J. Biol. Chem.* 234, 466-468.
- Boesze-Battaglia, K., & Albert, A. D. (1990) *J. Biol. Chem.* 265, 20727-20730.
- Boesze-Battaglia, K., Hennessey, T., & Albert, A. D. (1989) *J. Biol. Chem.* 264, 8151.
- Boesze-Battaglia, K., Fliesler, S. J., & Albert, A. D. (1990) *J. Biol. Chem.* 265, 18867-18870.
- Chen, L. A., Dale, R. E., Roth, S., & Brand, L. (1977) *J. Biol. Chem.* 252, 2163-2169.
- DeGrip, W. J., Gray, D., Gillespie, J., Bovee, P. H. M., Van den Berg, Lugtenberg, J., & Rothschild, K. J. (1988) *Photochem. Photobiol.* 48, 497-504.
- Drenthe, E. H. S., Klopmaekers, A. A., Bonting, S. L., & Daemen, F. J. M. (1981) *Biochim. Biophys. Acta* 641, 377-385.
- Emeis, D., Kuhn, H., Riechert, J., & Hofmann, K. P. (1982) *FEBS Lett.* 43, 29-34.
- Evans, E., & Needham, D. (1987) *J. Phys. Chem.* 91, 4219-4228.
- Hargrave, P. A., McDowell, J. H., Curtis, D. R., Wang, J. K., Juszczak, Fong, S.-L., Rao, J. K. M., & Argos, P. (1983) *Biophys. Struct. Mech.* 9, 235-244.
- Hildenbrand, K., & Nicolau, C. (1979) *Biochim. Biophys. Acta* 553, 365-377.
- Hong, K., & Hubbell, W. L. (1972) *Proc. Natl. Acad. Sci. U.S.A.* 69, 2617-2621.
- Jackson, M. L., & Litman, B. J. (1985) *Biochim. Biophys. Acta* 812, 369-376.
- Johnson, M. L. (1983) *Biophys. J.* 44, 101-106.
- Johnson, M. L. (1985) *Anal. Biochem.* 148, 471-478.
- Johnson, M. L., & Frazier, S. G. (1985) *Methods Enzymol.* 117, 301-342.
- Kariel, N., Davidson, E., & Keough, K. M. W. (1991) *Biochim. Biophys. Acta* 1062, 70-76.

- Kawato, S., Kinoshita, K., Jr., & Ikegami, A. (1977) *Biochemistry* 16, 2319-2324.
- Kibelbek, J., Mitchell, D. C., Beach, J., & Litman, B. J. (1991) *Biochemistry* 30, 6761-6768.
- Kinoshita, K., Jr., Kataoka, R., Kimura, Y., Gotoh, O., & Ikegami, A. (1981a) *Biochemistry* 20, 4270-4277.
- Kinoshita, K., Jr., Kawato, S., Ikegami, A., Yoshida, S., & Orii, Y. (1981b) *Biochim. Biophys. Acta* 647, 7-17.
- Klausner, R. D., Klienfeld, A. M., Hoover, R. L., & Karnovsky, M. J. (1980) *J. Biol. Chem.* 255, 1286-1295.
- Lakowicz, J. R. (1980) *J. Biochem. Biophys. Methods* 2, 91-119.
- Lakowicz, J. R., Cherek, H., Maliwal, B. P., & Gratton, E. (1985) *Biochemistry* 24, 376-383.
- Lamola, A. A., Yamane, T., & Zipp, A. (1974) *Biochemistry* 13, 738-745.
- Litman, B. J. (1982) *Methods Enzymol.* 81, 150-153.
- Litman, B. J., Kalisky, O., & Ottolenghi, M. (1981) *Biochemistry* 20, 631-634.
- Litman, B. J., Lewis, E. N., & Levin, I. W. (1991) *Biochemistry* 30, 313-319.
- Mathews, R. G., Hubbard, P. K., & Wald, G. (1963) *J. Gen. Physiol.* 47, 215-240.
- Miljanovich, G. P., Sklar, L. A., White, D. L., & Dratz, E. A. (1979) *Biochim. Biophys. Acta* 552, 294-306.
- Mitchell, D. C., Straume, M., Miller, J. L., & Litman, B. J. (1990) *Biochemistry* 29, 9143-9149.
- Mitchell, D. C., Kibelbek, J., & Litman, B. J. (1991a) *Biochemistry* 30, 37-42.
- Mitchell, D. C., Straume, M., & Litman, B. J. (1991b) *Biophys. J.* 59, 380a.
- Mone, A. P., & Litman, B. J. (1991) *Biophys. J.* 59, 621a.
- Moore, N. F., Patzer, E. J., Barenholz, Y., & Wagner, R. R. (1977) *Biochemistry* 16, 4708-4715.
- Needham, D., & Nunn, R. S. (1990) *Biophys. J.* 58, 997-1009.
- O'Brien, D. F., Costa, L. F., & Ott, R. A. (1977) *Biochemistry* 16, 1295-1303.
- Parasassi, T., Conti, F., Glaser, M., & Gratton, E. (1984) *J. Biol. Chem.* 259, 14011-14017.
- Sankaram, M. B., & Thompson, T. E. (1990) *Biochemistry* 29, 10676-10684.
- Slater, T. F. (1984) *Methods Enzymol.* 105, 283-293.
- Smith, H. G., Jr., Stubbs, G. W., & Litman, B. J. (1975) *Exp. Eye Res.* 20, 211-217.
- Straume, M., & Litman, B. J. (1987a) *Biochemistry* 26, 5121-5126.
- Straume, M., & Litman, B. J. (1987b) *Biochemistry* 26, 5113-5120.
- Straume, M., & Litman, B. J. (1988) *Biochemistry* 27, 7723-7733.
- Straume, M., Mitchell, D. C., Miller, J. L., & Litman, B. J. (1990) *Biochemistry* 29, 9135-9142.
- Stubbs, C. D., Kouyama, T., Kinoshita, K., Jr., & Ikegami, A. (1981) *Biochemistry* 20, 4257-4262.
- Stubbs, C. D., Kinoshita, K., Jr., Munkoge, F., Quinn, P. J., & Ikegami, A. (1984) *Biochim. Biophys. Acta* 755, 374-380.
- Sunamoto, J., Baba, Y., Iwamoto, K., & Kondo, H. (1985) *Biochim. Biophys. Acta* 833, 144-150.
- van de Ven, M., van Ginkel, G., & Levine, Y. K. (1984) *Biochem. Biophys. Res. Commun.* 123, 352-357.
- Vogel, H., & Jahnig, F. (1985) *Proc. Natl. Acad. Sci. U.S.A.* 82, 2029-2033.
- Vos, M. H., Kooyman, R. P. H., & Levine, Y. K. (1983) *Biochem. Biophys. Res. Commun.* 116, 462-468.
- Wiedmann, T. S., Pates, R. D., Beach, J. M., Salmon, A., & Brown, M. F. (1988) *Biochemistry* 27, 6469-6474.